Date of publication xxxx 00, 0000, date of current version xxxx 00, 0000.

Digital Object Identifier 10.1109/ACCESS.2017.DOI

Coordinate Transformation-Free Observer-based Adaptive Estimation of Distorted Single-Phase Grid Voltage Signal

HAFIZ AHMED[1], (Member, IEEE), MOMINUL AHSAN [2], MOHAMED BENBOUZID [3,6], (Fellow, IEEE), ALHUSSEIN ALBARBAR [2], MOHAMMAD SHAHJALAL [4], and SAMET BIRICIK[5,7], (Senior Member, IEEE)

[1]School of Mechanical, Aerospace and Automotive Engineering, Coventry University, UK (e-mail: hafiz.h.ahmed@ieee.org).
[2]Smart Infrastructure and Industry Research Group, John Dalton Building, Department of Engineering, Manchester Metropolitan University, Chester St, Manchester M1 5GD, UK (e-mail: a.albarbar,m.ahsan@mmu.ac.uk).
[3]University of Brest, UMR CNRS 6027 IRDL, 29238 Brest, France (e-mail: mohamed.benbouzid@univ-brest.fr).
[4]Warwick Manufacturing Group (WMG), University of Warwick, Coventry, UK (e-mail: Mohammad.Shahjalal@warwick.ac.uk).
[5]Department of Electrical and Electronics Engineering, European University of Lefke, Lefke, Northern Cyprus, TR-10 Mersin, Turkey (e-mail: sbiricik@eul.edu.tr).
[6]Logistics Engineering College, Shanghai Maritime University, 201306 Shanghai, China.
[7]School of Electrical and Electronic Engineering, Technological University Dublin, Dublin, Ireland.

Corresponding author: Mominul Ahsan (e-mail: m.ahsan@mmu.ac.uk).

The research presented in this paper has received financial support from the Manchester Met University (MMU)

ABSTRACT This paper studies the phase and frequency estimation problem of single-phase grid voltage signal in the presence of DC offset and harmonics. For this purpose, a novel parameterized linear model of the grid voltage signal is considered where the unknown frequency of the grid is considered as the parameter. Based on the developed model, a linear observer (Luenberger type) is proposed. Then using Lyapunov stability theory, an estimator of the unknown grid frequency is developed. In order to deal with the grid harmonics, multiple parallel observers are then proposed. The proposed technique is inspired by other Luenberger observers already proposed in the literature. Those techniques use coordinate transformation that requires real-time matrix inverse calculation. The proposed technique avoids real-time matrix inversion by using a novel state-space model of the grid voltage signal. In comparison to similar other techniques available in the literature, no coordinate transformation is required. This significantly reduces the computational complexity w.r.t. similar other techniques. Comparative experimental results are provided with respect to two other recently proposed nonlinear techniques to show the dynamic performance improvement. Experimental results demonstrate the suitability of the proposed technique.

INDEX TERMS Frequency Estimation, Phase Estimation, State Estimation, Power System Measurements, Observers, Nonlinear Systems, Adaptive Estimation, Harmonic Distortion

I. INTRODUCTION

Phase angle and frequency play an important role in the control of grid-connected systems e.g. inverters [1]–[5], dynamic voltage restorer [6], rectifier [7], [8], to name a few. All these applications require an estimator that can converge in few cycles and have good steady-state performance in the presence of various disturbances and uncertainties. To meet this demand, numerous solutions have been proposed in the literature such as discrete Fourier transform (DFT) [9], various variants of Kalman filter [10], [11], various variants of least-square estimation [12], [13], adaptive notch filter (ANF) [14], various variants of delayed signal cancellation (DSC) techniques [15]–[19], linear observer [20]–[23], harmonic oscillators (linear and nonlinear) [24], [25], various variants of phase-locked loop (PLL) [26]–[30], demodulation-based techniques [31], [32], open-loop techniques [33], [34], etc.

DFT based technique as reported in [9] is an useful approach. However the presence of harmonics increases the computational burden enormously as large window size

is required. Moreover, numerous parameters need to be tuned. Kalman filter based techniques [10], [11] overcome the problem of tuning numerous parameters. But it uses coordinate transformation to transform the system dynamics from the state matrix to the output matrix one. This increases the computational burden. Moreover, online computation of matrix inverse is also required. Linear observers proposed in [20]–[23] use similar dynamic model as used by Kalman filter. However, linear observers also uses coordinate transformation. Moreover, as phase angle can be obtained only in the original coordinate, matrix inverse is required to return back to the original coordinates. As a result the overall computational burden is high. Kalman filter [10] uses similar dynamic model as that of adaptive observer. It has excellent noise filtering property. However, it uses dynamic gains as opposed to fixed observer gains used in adaptive observer. The dynamic gains are obtained at each time instant by computation matrix inverse. This is computationally demanding. Computational burden is also an issue for least-square estimation based techniques [12], [13]. To overcome the high computational burden, adaptive notch filter (ANF) [14] can be a good alternative. By filtering out the higher order harmonics, an accurate estimation of the grid frequency can be obtained by ANF. Delayed signal cancellation (DSC) is another technique that become popular in recent time. DSC-based open and closed-loop grid synchronization techniques are reported in [15]–[19]. DSC-based techniques generally show excellent performances, however, they have high memory requirement to implement the delayed signal. This could be a limiting factor in implementing DSC-based techniques in low-cost micro-controllers.

Out of various techniques, PLL [26]–[30] received wide spread attention due to its excellent performances yet having a simple structure. However, in the case of simple PLL, there is a trade-off between disturbance rejection capability and fast dynamic response. To overcome this trade-off, numerous modifications are proposed. Modified or Enhanced PLLs [35] generally have good dynamic performance with respect to traditional PLLs but comes at a cost of higher computational resources. Moreover, small oscillations may also be observed in the presence of non-ideal frequency and DC offset. Second order generalized integrator - frequency-locked loop (SOGI-FLL) [24] and its various linear and nonlinear variants are another type popular technique widely used in the literature. The presence of FLL block makes the overall system nonlinear. However, as the fundamental block of this technique uses a linear harmonic oscillator, the presence of harmonics will give rise to steady-state error. Using filter similar to SOGI, [34] proposed a pseudo-open loop technique for three-phase system. This result can be easily adapted to single-phase system using orthogonal signal generator (OSG). This technique uses derivative of the signals to estimate frequency. This can limit the application in noisy environment as derivative amplifies the noise.

Demodulation is another type of technique [31], [32] that got some attention in recent time. Using signal mixing, this technique generate constant signals for frequency estimation purpose. Demodulation has good dynamic performance and disturbance rejection capability. However, it is computationally expensive as at least three trigonometric functions are used.

In this paper, a novel time-domain technique for the estimation of the phase and frequency of single-phase grid voltage signal is proposed. The proposed technique can work in the presence of DC offset and harmonics. In comparison to the other time-domain techniques, no complex filtering or quadrature signal generator (QSG) is required. Instead, the grid voltage system is considered as a time-varying dynamical systems. Then a frequency adaptive observer for this dynamical system is designed. The proposed approach is easy to use and implement. Finally, using linearization-based approach, stability analysis is also provided.

The contributions of this paper are threefold. Firstly, a novel state-space model of the grid voltage system is proposed. To the best of the author's knowledge, such a model does not exist in the grid voltage parameter estimation literature. Moreover, the model explicitly considers DC offset. Secondly, thanks to the novel state-space model, no need of coordinate transformation unlike [20]–[23]. The inverse of a $n \times n$ matrix requires n^3 multiplications/divisions and $n^3 - 2n^2 + n$ additions/subtractions operations [36]. These mathematical operations are not required by the proposed technique. This is a significant computational advantage over the existing literature. Finally, a simple computational procedure for the gain tuning is proposed.

The rest of the paper is organized as follows: The proposed approach is given in Sec. II. Extension of the proposed approach to harmonics is given in Sec III. Experimental results are given in Sec. IV. Finally Sec. V concludes this paper.

II. ESTIMATION OF PHASE AND FREQUENCY

The grid voltage signal is presented by:

$$y = v_d + \nu_g \sin \underbrace{(\omega t + \varphi)}_{\theta} \tag{1}$$

where ν_g is the amplitude, $\omega = 2\pi f$ is the unknown angular frequency with f being the frequency, φ is the phase and $\theta \in [0, 2\pi)$ is the unknown instantaneous phase and $v_d, |v_d| \geq 0$ is the DC bias/offset of the grid voltage signal. In this paper, the problem being considered is to estimate f and θ in the presence of various disturbances and uncertainties e.g. non-smooth jump of phase, frequency, DC offset and amplitude. In the traditional state space observer design [20]–[22], by considering $y = x_1$, and $\dot{y} = x_2$, the dynamics of the grid voltage signal in the state-space form is given by:

$$\dot{x} = \bar{A}x \tag{2a}$$
$$y = \bar{C}x \tag{2b}$$

where

$$x = \begin{bmatrix} x_1 \\ x_2 \\ x_3 \end{bmatrix} = \begin{bmatrix} \nu_g \sin(\theta) \\ \nu_g \omega \cos(\theta) \\ v_d \end{bmatrix},$$
$$\bar{A} = \begin{bmatrix} 0 & 1 & 0 \\ -\omega^2 & 0 & 0 \\ 0 & 0 & 0 \end{bmatrix}, \bar{C} = \begin{bmatrix} 1 & 0 & 1 \end{bmatrix}$$

with $\omega^2 = \mu\omega_n^2, \mu > 0, \omega_n = 100\pi$. With the chosen state variables, estimating x_2 from y is essentially estimating the derivative of y. As the derivative is ω times the actual signal, from the numerical point of view, it is very difficult to estimate x_2 from x_1. As such time-varying coordinate transformations are widely used in the literature to transform the system dynamics from the state matrix $\bar{A}$ to to the output matrix $\bar{C}$. Although all the calculations are done in the transformed system, parameter like θ can often only be obtained in the original coordinates. As such inverse transformation is required, the overall computational burden increases dramatically. For low-cost hardware this is a big challenge. For expensive hardware, this can be a bottleneck to achieve higher sampling frequency as is required for several applications e.g. control of high switching frequency inverter.

To overcome the above-mentioned computational complexity problem associated with the coordinate transformation, in this paper, a new state variable $\frac{-\nu_g}{\omega}\cos(\theta)$ is introduced to transform the problem of derivative estimation into a problem of integration. This helps to avoid the computationally expensive coordinate transformation. In the new states, the dynamics of the grid voltage can be written as:

$$\dot{z} = Az \tag{3a}$$
$$y = Cz \tag{3b}$$

where

$$z = \begin{bmatrix} z_1 \\ z_2 \\ z_3 \end{bmatrix} = \begin{bmatrix} -\frac{\nu_g}{\omega}\cos(\theta) \\ \nu_g \sin(\theta) \\ v_d \end{bmatrix}, C = \begin{bmatrix} 0 & 1 & 1 \end{bmatrix}$$

while $A = \bar{A}$. Then the following Luenberger observer is designed for system (3):

$$\dot{\hat{z}} = \hat{A}\hat{z} + L\left(y - C\hat{z}\right) \tag{4}$$
$$\dot{\hat{\mu}} = -\omega_n^2 \hat{z}_1 |y - C\hat{z}|^{\alpha} \tanh\left\{k\left(y - C\hat{z}\right)\right\} \tag{5}$$

where, k and α are positive constants to be tuned, $\hat{z}$ is the estimation of z,

$$\hat{A} = \begin{bmatrix} 0 & 1 & 0 \\ -\hat{\mu}\omega_n^2 & 0 & 0 \\ 0 & 0 & 0 \end{bmatrix}, L = \begin{bmatrix} l_1 \\ l_2 \\ l_3 \end{bmatrix},$$

and $\dot{\hat{\mu}}$ is the updating law for the unknown frequency estimation. If the grid frequency is known *i.e.* $\mu = \hat{\mu}$, then for properly selected matrix L i.e. $\mathcal{R}\{\lambda(A - LC)\} < 0$, the convergence of the observer (4) is guaranteed. In this paper, it is assumed that the grid frequency is unknown constant and slowly time-varying i.e. $\dot{\mu} = 0$. As such the convergence is not guaranteed in this case. Frequency update law (5) is designed to ensure the convergence of the observer in the presence of unknown frequency.

Let us consider the observer estimation error as

$$\begin{aligned}
\varepsilon &= z - \hat{z} \\
\dot{\varepsilon} &= \dot{z} - \dot{\hat{z}} \\
&= Az - \left\{\hat{A}\hat{z} + L(y - C\hat{z})\right\} \\
&= Az - A\hat{z} + A\hat{z} - \hat{A}\hat{z} - L(Cz - C\hat{z}) \\
&= (A - LC)(z - \hat{z}) + \left(A - \hat{A}\right)\hat{z} \\
&= (A - LC)\varepsilon \\
&+ \left(\begin{bmatrix} 0 & 1 & 0 \\ -\mu\omega_n^2 & 0 & 0 \\ 0 & 0 & 0 \end{bmatrix} - \begin{bmatrix} 0 & 1 & 0 \\ -\hat{\mu}\omega_n^2 & 0 & 0 \\ 0 & 0 & 0 \end{bmatrix}\right)\begin{bmatrix} \hat{z}_1 \\ \hat{z}_2 \\ \hat{z}_3 \end{bmatrix}
\end{aligned}$$

$$\dot{\varepsilon} = (A - LC)\varepsilon - \underbrace{\begin{bmatrix} 0 \\ 1 \\ 0 \end{bmatrix}}_{B} \underbrace{(\mu - \hat{\mu})}_{\varepsilon_\mu} \omega_n^2 \hat{z}_1 \tag{6}$$

Moreover, the parameter estimation dynamics is given by:

$$\begin{aligned}
\dot{\varepsilon}_\mu &= \dot{\mu} - \dot{\hat{\mu}} \\
\dot{\varepsilon}_\mu &= \omega_n^2 \hat{z}_1 |y - C\hat{z}|^{\alpha} \tanh\left\{k\left(y - C\hat{z}\right)\right\}
\end{aligned} \tag{7}$$

The desired equilibrium of the state and parameter estimation error is given by

$$x^\star = \{\varepsilon = 0, \varepsilon_\mu = 0, \mu = \hat{\mu} = 1\}$$

Linearization of the state and parameter estimation error dynamics (eq. (6) and (7)) with respect to the desired equilibrium gives rise to Jacobian matrix:

$$J(x^\star) = \begin{bmatrix} 0 & 1 - l_1 & -l_1 & 0 \\ -\omega_n^2 & -l_2 & -l_2 & -\omega_n^2 \hat{z}_1 \\ 0 & -l_3 & -l_3 & 0 \\ 0 & 0 & 0 & 0 \end{bmatrix} \tag{8}$$

Local stability of the closed-loop system depends on the eigenvalues of $J(x^\star)$. This can be obtained from the following characteristics equation

$$s^4 + (l_2 + l_3)s^3 + (\omega_n^2 - l_1\omega_n^2)s^2 + l_3\omega_n^2 s + 0s^0 = 0 \tag{9}$$

Eigenvalues of $J(x^\star)$ are the roots of Eq. (9). Real parts of the roots are non-positive if all the coefficients of polynomial (9) are non negative. If we select $l_1 < 0$ and $l_2, l_3 > 0$, then all the coefficients of the polynomial (9) are

Table 1: ROUTH HURWITZ TABLE.

s^4	1	$\omega_n^2(1-l_1)$	0	0	0
s^3	l_2+l_3	$l_3\omega_n^2$	0	0	0
s^2	$-\frac{\{(l_2+l_3)(l_1-1)+l_3\}\omega_n^2}{l_2+l_3}$	0	0	0	0
s^1	$l_3\omega_n^2$	0	0	0	0

non-negative. Non-negative coefficients are necessary but not sufficient to show that the matrix $J(x^\star)$ is Hurwitz stable as the polynomial order is greater than 2. For this Routh-Hurwitz test needs to be considered. Routh-Hurwitz table for polynomial (9) is given in Table 1. If the parameters are chosen as $l_1 < 0$ and $l_2 + l_3 > l_3$ with $l_2, l_3 > 0$, then there is no sign change in the second column of Table 1, then the polynomial (9) is Hurwitz stable. Since one of the roots is zero for polynomial (9), the closed-loop system is marginally stable. To show the exact convergence of the parameter estimation i.e. $\varepsilon_\mu = 0$, let us consider the equilibrium point $\varepsilon = 0$. Then from the observer error dynamics (6), and the parameter identification law (5), it can be written that

$$\varepsilon_\mu \hat{z}_1 = 0 \qquad \text{and} \quad \dot{\varepsilon}_\mu = 0 \tag{10}$$

Since $\varepsilon_1 = z_1 - \hat{z}_1 = 0$ and $z_1 = -\frac{\nu_g}{\omega}\cos(\theta)$, then

$$\varepsilon_\mu \hat{z}_1 = \varepsilon_\mu z_1 = \varepsilon_\mu \gamma \cos(\theta) = 0 \tag{11}$$

where $\gamma = -\frac{v_g}{\omega} \neq 0$. By taking derivative on (11), one can get

$$-\varepsilon_\mu \gamma \sin(\theta) = 0 \tag{12}$$

It is clear that $\gamma, \cos(\theta), \sin(\theta) \neq 0, \forall t$, Then from eq. (11) and (12), it can be clearly inferred that $\varepsilon_\mu = 0$. This actually completes the local asymptotic stability of the proposed adaptive observer.

A. REMARKS ON THE TUNING OF OBSERVER GAIN L

Let us assume that the desired closed-loop poles are $\lambda_1 = -\omega_1 = -a\omega_n$, $\lambda_2 = -\omega_2 = -b\omega_n$ and $\lambda_3 = -\omega_3 = -c\omega_n$. Then, the gain L can be found by solving the following equation:

$$\begin{aligned} |sI_3 - (A_{\mu=1} - LC)| &= (s+\omega_1)(s+\omega_2)(s+\omega_3) \\ s^2 + (l_2+l_3)s^2 + \omega_n^2(1-l_1)s + l_3\omega_n^2 &= s^3 + \\ (a+b+c)\omega_n s^2 + (ab+bc+ca)\omega_n^2 s + abc\omega_n^3 \end{aligned} \tag{13}$$

By equating the coefficients of (13), one can easily find the gains of the observer as,

$$l_1 = 1-(ab+bc+ca),\ l_2 = (a+b+c-abc)\omega_n, l_3 = abc\omega_n \tag{14}$$

In tuning the observer gains, it has to be noted that DC offset appears as a pure integrator in the grid voltage model (3). Following the results available in [37], convergence of the DC offset estimation part should be slower than the grid voltage estimation part i.e. $|\lambda_2| < |\lambda_3|$. Otherwise, numerical instability and/or oscillation in the estimated value may appear.

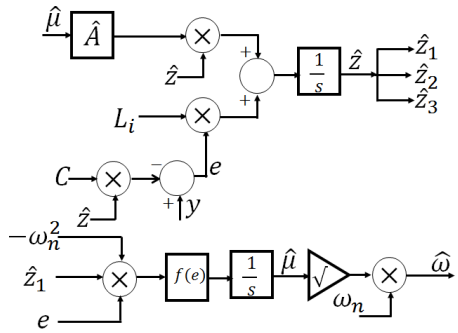

Figure 1: Block diagram of the proposed adaptive observer (AO), harmonics free case.

Using the estimated $\hat{\mu}$, the frequency and the phase can be calculated by:

$$\hat{f} = \frac{\sqrt{\hat{\mu}}\omega_n}{2\pi} \tag{15a}$$

$$\hat{\theta} = \arctan\left(\frac{\hat{z}_2}{-\hat{\omega}\hat{z}_1}\right) \tag{15b}$$

To implement the proposed adaptive observer-based phase and frequency estimation technique, Eq. (4), (5) and (15) are required. Block diagram of the proposed observer is given in Fig. 1.

B. STEP-BY-STEP DESIGN PROCEDURE

This Section summarizes the design procedure for the proposed technique when only the observer tuned at fundamental frequency is considered. The design process considers the following two steps:

- Step-1: Observer gain matrix L selection for eq. (4).
- Step-2: Frequency update law parameters selection for eq. (5).

As shown in Sec. II-A, in this paper, we consider pole placement-based observer gain tuning. For this purpose, desired poles of the closed-loop system need to be selected. To do this, let us consider the open-loop poles of matrix $A = \hat{A}_{\mu=1}$ which are $0, \pm j\omega$. Then, the observer gain matrix L needs to be selected in a way that will ensure the closed-loop error system matrix $\hat{A} - LC$ have negative real parts. Potential choice of closed-loop poles are given in eq. (20) (Sec. IV). Then, by substituting the value of desired closed-loop poles λ_1, λ_2, and λ_3 in eq. (14), the observer gain matrix $L = [l_1\ l_2\ l_3]^T$ can be found. Alternatively, the command `place` in Matlab can also be used. The next step is to tune the frequency identification parameters k and α. The frequency update law (5) is highly nonlinear. As such, obtaining a simple tuning rule is not straightforward. These parameters can be tuned using trial and error. For this purpose, one can first select the gain α between 0.1 and 2.

Then, the gain k can be iteratively obtained. This completes the design process.

III. MULTIPLE ADAPTIVE OBSERVER

In Sec. II, only the fundamental frequency case is considered. In the presence of harmonics, observer (4) will have steady-state error. To overcome this problem, there are two potential solutions. One solution would be to consider higher order system considering harmonics. The order of the system will be $2n+1$ where n is the number of harmonic components. Tuning the gain matrix L for such a high order system with desired precision is not straightforward. Another solution is to consider multiple adaptive observer (4) tuned at different frequencies. Since the frequencies are odd multiple of the fundamental frequency, only one frequency update law is sufficient. Mathematically multiple adaptive observer (MAO) in this case can be represented as for $i = 1, 2, ..., n$:

$$\dot{\hat{z}}_i = \hat{A}_i \hat{z}_i + L_i e, \tag{16a}$$

$$e = y - C\hat{\bar{z}}, \tag{16b}$$

$$\dot{\hat{\mu}} = -\omega_n^2 \hat{z}_{11} \underbrace{|e|^{\alpha} \tanh\{ke\}}_{f(e)}, k, \alpha > 0 \tag{16c}$$

where for $i = 2, ..., n$

$$\hat{z}_i = [\hat{z}_{1i}\ \hat{z}_{2i}]^T, \hat{z}_1 = [\hat{z}_{11}\ \hat{z}_{21}\ \hat{z}_3]^T,$$
$$\hat{\bar{z}} = [\hat{z}_1\ \hat{z}_2 ...\ \hat{z}_n],$$
$$C = [0\,1\,1\,0\,1\,0 ...\ 0\,1],$$
$$\hat{A}_i = \begin{bmatrix} 0 & 1 \\ -\hat{\mu}\omega_i^2 & 0 \end{bmatrix}, \hat{A}_1 = \begin{bmatrix} 0 & 1 & 0 \\ -\hat{\mu}\omega_n^2 & 0 & 0 \\ 0 & 0 & 0 \end{bmatrix}$$

with $\omega_i = (2i-1)\omega_n$. For properly tuned observer gain matrix L_i, individual observers are stable. As a result, bounded input bounded output (BIBO) stability of the proposed multiple adaptive observer can be established using Theorem 2 given in [38]. Moreover, the boundedness and exponential decay of the signal estimation error can be established using Theorem A.3 given in [38]. It is to be noted here that this result is mathematically weaker than the global exponential stability results presented in [21], [22].

Using the estimated $\hat{\mu}$, the frequency and the phase of the fundamental components can be calculated by:

$$\hat{f} = \frac{\sqrt{\hat{\mu}}\omega_n}{2\pi} \tag{17a}$$

$$\hat{\theta} = \arctan\left(\frac{\hat{z}_{22}}{-\hat{\omega}\hat{z}_{12}}\right) \tag{17b}$$

Tuning of the observer gains L_i can be performed using the same ideas presented in Sec. II-A. To implement the proposed multiple adaptive observer-based phase and frequency estimation technique, Eq. (16) and (17) are required. Block diagram of the proposed observer is given in Fig. 2.

The design process in this case is similar to Sec. II-B. Here, instead of one observer, multiple observers need to

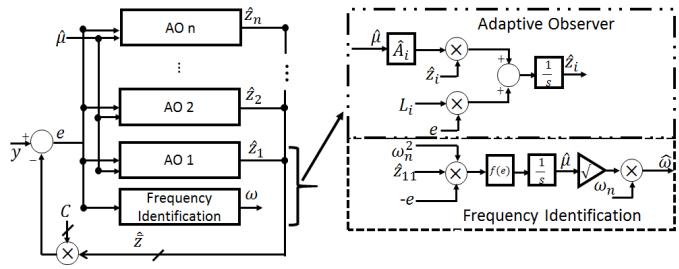

Figure 2: Block diagram of the proposed multiple adaptive observer (MAO).

be tuned. However, the tuning formula remains the same for the observer tuned at the fundamental frequency. To tune the observers for harmonic frequencies, let us assume that the desired closed-loop poles for the harmonic observers are $\lambda_{1i} = -a_i\omega_i$ and $\lambda_{2i} = -b_i\omega_i$, where $i = 2, ..., n$ and $\omega_i = (2i-1)$. Then, the gain $L_i = [l_{1i}\ l_{2i}]^T$ can be found by solving the following equation:

$$|sI_2 - ((A_i)_{\mu=1} - L_i C_i)| = (s + a_i\omega_i)(s + b_i\omega_i)$$
$$s^3 + l_{2i}s + \omega_i^2(1 - l_1) = s^2 + (a_i + b_i)\omega_i s + a_i b_i \omega_i^2 \tag{18}$$

where $C_i = [0 \quad 1]$. By equating coefficients of (18), one can easily find the observer gain as,

$$l_{1i} = 1 - a_i b_i, \quad l_{2i} = (a_i + b_i)\omega_i \tag{19}$$

IV. RESULTS AND DISCUSSIONS

A. HARDWARE-IN-THE-LOOP (HIL) EXPERIMENTAL RESULTS

To validate the theoretical results of Sec. II, dSPACE 1104 board-based hardware-in-the-loop (HIL) experimental results are considered. For this purpose, the proposed adaptive observer (AO) is implemented in Matlab/Simulink using Runge-Kutta discretization technique with a sampling frequency of 10kHz. As a comparison tool, circular limit cycle oscillator - frequency-locked loop (CLO) [39] and adaptive notch filter (ANF) [14] are selected. Both of the comparison techniques are nonlinear in nature and can handle DC bias. They have been selected for their superiority over state-of-the-art techniques.

Proposed AO have three parameters to tune, observer gain matrix L and k, α in Eq. (5). Tuning of L has been discussed in Sec. II-A. The first step in tuning the gain is to select the desired poles of the closed-loop observer error system. The poles are selected as

$$(\lambda_{z_1}, \lambda_{z_2}, \lambda_{z_3}) = \left(-\underbrace{0.4597}_{a}\omega_n, -\underbrace{1.7403}_{b}\omega_n, -\underbrace{1}_{c}\omega_n\right) \tag{20}$$

with $\omega_n = 100\pi$. The closed-loop poles can be selected arbitrarily. From the desired pole locations, observer gain matrix $L = [l_1\ l_2\ l_3]^T$ can be selected as:

$$l_1 = 1 - (ab + bc + ca) = -2$$
$$l_2 = (a + b + c - abc)\omega_n = 2.4\omega_n$$
$$l_3 = abc\omega_n = 0.8\omega_n$$

Frequency identification gain α and k are nonlinearly related with the output estimation error and $\hat{z}_1$. As such obtaining any analytical tuning rule is difficult. Through extensive numerical simulation it has been found that higher values of α decreases the peak estimation error but increases the convergence time whereas higher values of α does the opposite. So, α can be selected as a trade-off between fast convergence and satisfactory steady-state responses. It has been found that α can be selected anywhere between 0.1 and 2. The value of α is chosen accordingly. The other parameter k actually is used to approximate the sign function i.e $\text{sign}(e) \approx \tanh(ke)$. So, the choice of k is up to the designer. For sufficiently high values of k, chattering or high frequency oscillation might be introduced in the frequency identification part. As such lower values are recommended. Parameters of the comparative techniques are selected according to the guidelines in the original papers where the methods were proposed [14], [39].

To analyze the performance of the proposed AO, the following tests have been performed:

- Test-I: -2 Hz. frequency step change
- Test-II: -20° phase step change
- Test-III: $+0.2$ p.u. amplitude step change
- Test-IV: -0.1 p.u. DC offset step change

Comparative HIL experimental results are shown in Fig. 3, 4, 5, and 6 respectively . Comparative performances are summarized in Table 2 and 3. Four tests have been performed and the three criteria have been used to determine the performance of individual techniques. Out of 11 check boxes, AO ticked the box in eight cases which is approximately 75%. In every cases, AO had the lowest convergence time for both phase and frequency in addition to the lowest peak phase estimation error. The only area where AO did not outperform the comparative techniques is the peak frequency estimation error. It had lowest peak frequency estimation error only for the frequency step test. In other cases, the errors were a bit higher compared to the other techniques. This can be considered as a trade-off between fast dynamic response and peak estimation error. In many power electronic applications, only phase is being used (e.g. $\alpha\beta \rightarrow dq$ transformation). In that sense, proposed observer is significantly better than the selected comparative techniques. AO not only had the lowest phase estimation error but also had convergence time approximately two times faster. Overall, experimental results demonstrate the effectiveness of the proposed AO over other advanced nonlinear techniques.

Test I-IV assumed harmonics-free grid. This may not be the case always. To assess the performance of the proposed observer under harmonics, another test has been performed.

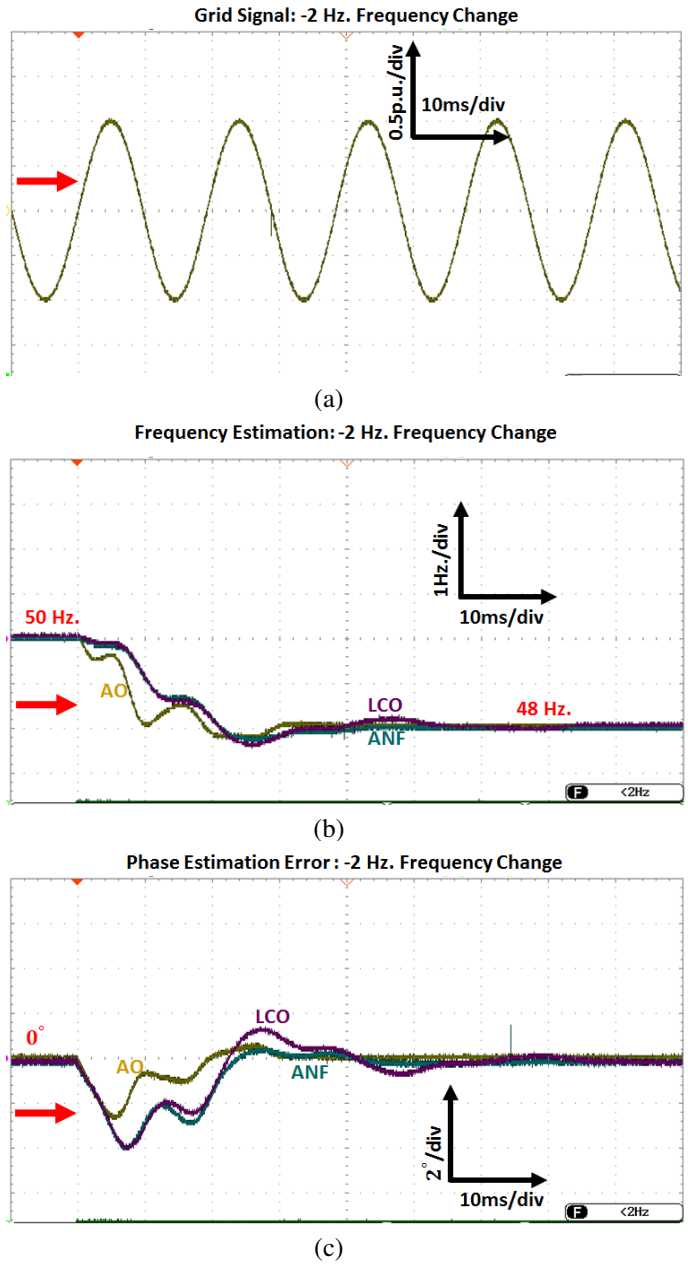

Figure 3: Comparative HIL experimental results for Test-I: -2 Hz step change in frequency, (a) Grid voltage signal, (b) Estimated frequencies, and (c) Phase estimation errors.

In this case, the grid signal is corrupted with 20% total harmonic distortion (THD) comprising 3rd, 5th, and 7th order harmonics each having an amplitude of 0.1155 p.u. HIL experimental results for MAO can be seen in Fig. 7. Figure 7 shows that MAO converged very fast with zero steady-state error for both phase and frequency estimations. The main purpose of this test is to demonstrate that extension of AO i.e. MAO can be applied for harmonics case also. For this reason, the comparative techniques are not included in this case.

Table 2: BEST PERFORMING TECHNIQUE COMPARATIVE SUMMARY FOR TEST SCENARIOS I, II, III, AND IV.

Step Change↓	Fastest Convergence Time (Freq. and Phase)			Lowest Peak Phase Error			Lowest Peak Frequency error		
	AO	CLO	ANF	AO	CLO	ANF	AO	CLO	ANF
Test-I: -2 Hz frequency	✓	✗	✗	✓	✗	✗	✓	✗	✓
Test-II: -20° phase	✓	✗	✗	NA	NA	NA	✗	✗	✓
Test-III: 0.2 p.u. amplitude	✓	✗	✗	✓	✗	✗	✗	✗	✓
Test-IV: -0.1 p.u. DC	✓	✗	✗	✓	✗	✓	✗	✗	✓

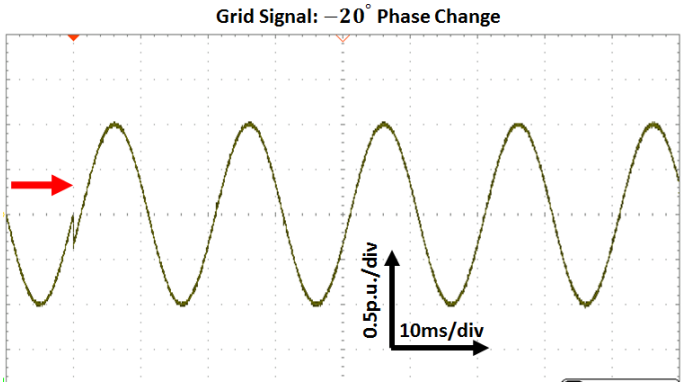

(a)

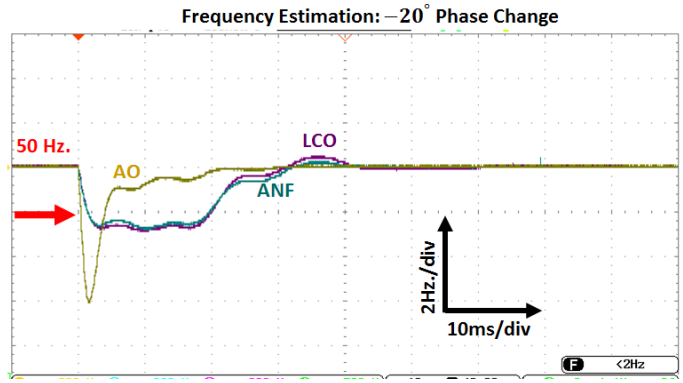

(b)

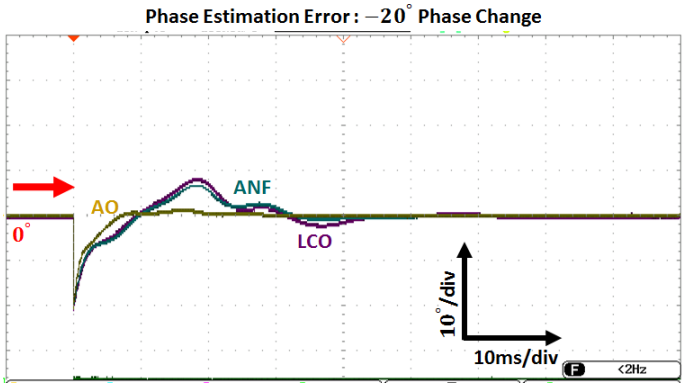

(c)

Figure 4: Comparative HIL experimental results for Test-II: -20° step change in phase, (a) Grid voltage signal, (b) Estimated frequencies, and (c) Phase estimation errors.

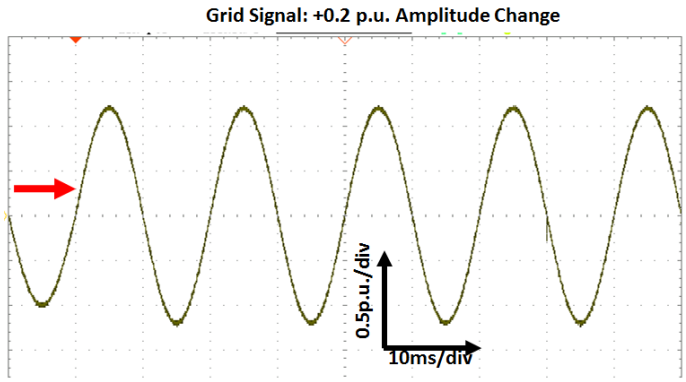

(a)

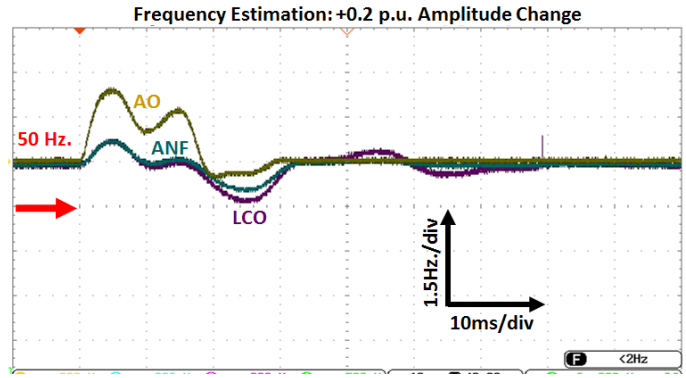

(b)

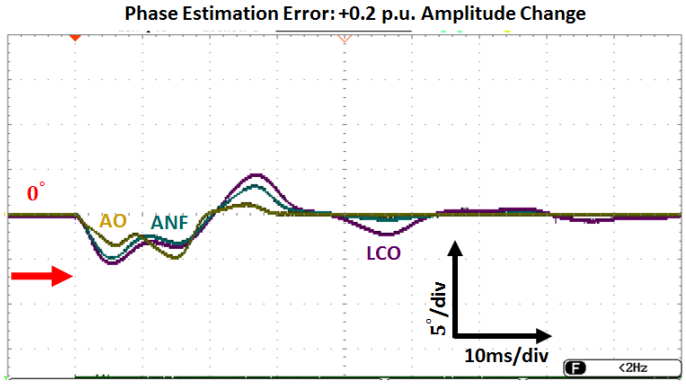

(c)

Figure 5: Comparative experimental results for Test III: $+0.2$p.u. step change in amplitude, (a) Grid voltage signal, (b) Estimated frequencies, and (c) Phase estimation errors.

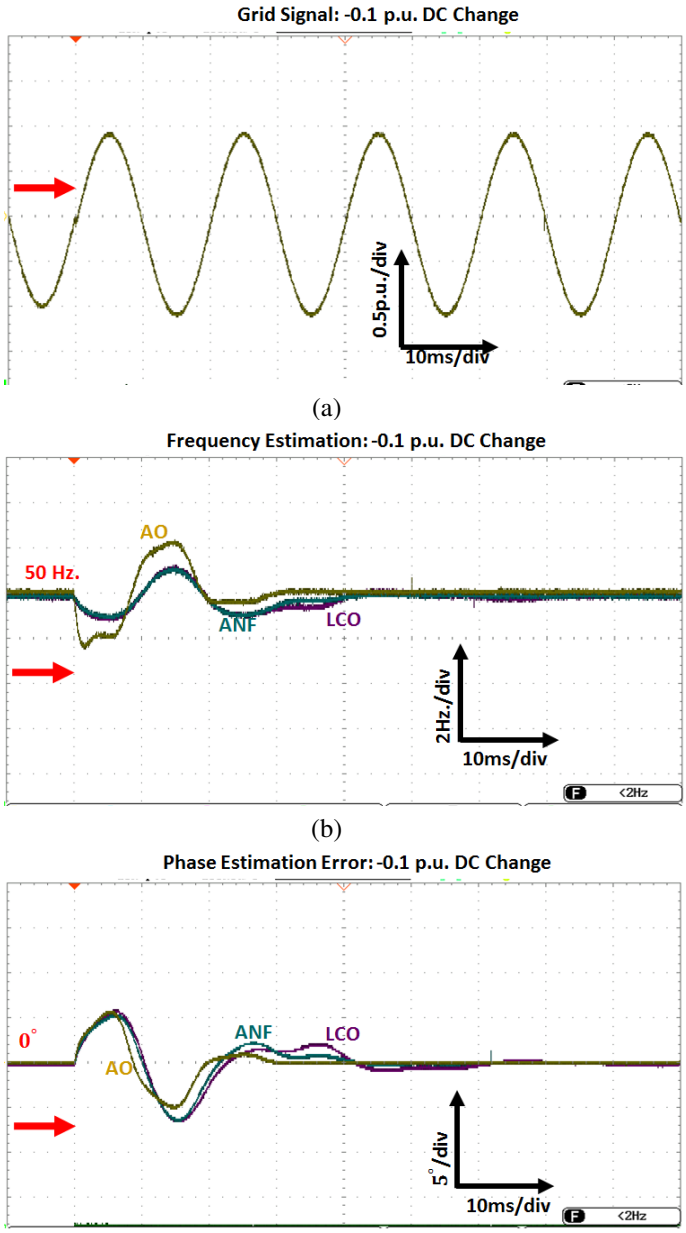

Figure 6: Comparative experimental results for Test-IV: -0.1 p.u. step change in DC bias, (a) Grid voltage signal, (b) Estimated frequencies, and (c) Phase estimation errors.

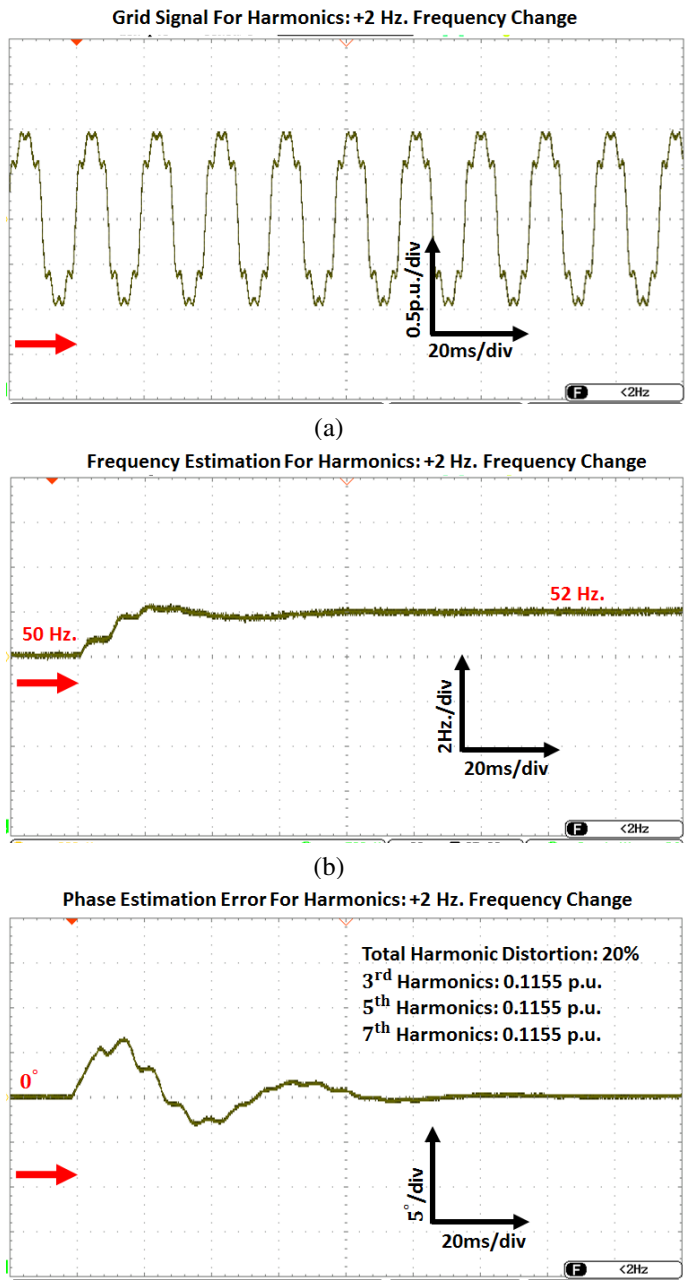

Figure 7: Comparative experimental results for 20% THD with 3rd, 5th, and 7th order harmonics each having an amplitude of 0.1155 p.u, (a) Grid voltage signal, (b) Estimated frequency, and (c) Phase estimation error.

B. EXPERIMENTAL RESULTS

In this Section, experimental study is considered. The experimental setup used in this work is given in Fig. 8. In the setup, a DC motor is coupled to a synchronous generator to emulate the adverse grid voltage conditions and the generated voltage at the load terminal is measured by using LEM LV25-P sensor with associated offset circuit. The experimental data of the grid voltage is processed by using a Texas Instruments TMS320F28335 digital signal processor. The sampling frequency is set to 10 kHz. The studied

Table 3: COMPARATIVE TIME DOMAIN PERFORMANCE SUMMARY.

	AO	CLO	ANF
-2 Hz. freq. change			
Freq. Settling time (± 0.1 Hz)	27 ms	30 ms	28 ms
Phase Settling time ($\pm 1^{\circ}$)	9 ms	20 ms	21 ms
Frequency overshoot	0.23 Hz	0.4 Hz	0.23 Hz
Phase overshoot	2.65°	3.85°	3.8°
$+20^{\circ}$ Phase change			
Freq. Settling time (± 0.1 Hz)	17 ms	38 ms	30 ms
Phase Settling time ($\pm 1^{\circ}$)	18 ms	40 ms	31 ms
Frequency overshoot	6 Hz	2.95 Hz	2.8 Hz
$+0.2$ p.u. amplitude change			
Freq. Settling time (± 0.1 Hz)	27 ms	78 ms	48 ms
Phase Settling time ($\pm 1^{\circ}$)	18 ms	50 ms	31 ms
Frequency overshoot	3 Hz	1.6 Hz	1.15 Hz
Phase overshoot	4.7°	5.3°	4.85°
-0.1 p.u. DC change			
Freq. Settling time (± 0.1 Hz)	28 ms	49 ms	38 ms
Phase Settling time ($\pm 1^{\circ}$)	18 ms	39 ms	31 ms
Frequency overshoot	2.35 Hz	1.25 Hz	1.16 Hz
Phase overshoot	5.6°	5.7°	5.6°

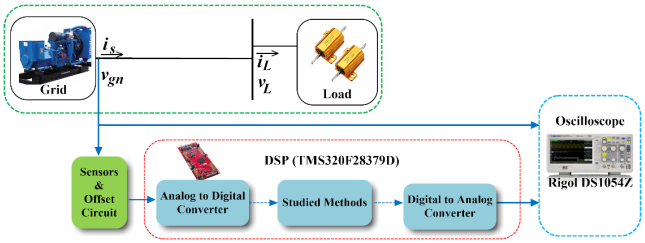

(a)

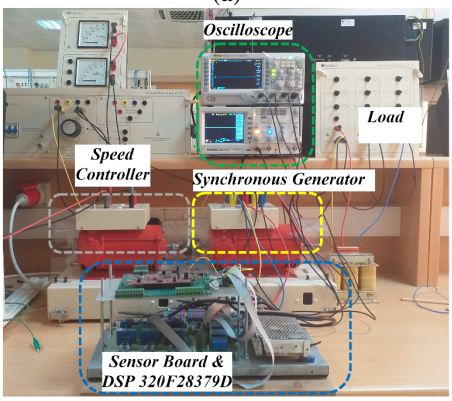

(b)

Figure 8: Experimental setup considered in this work - (a) Block diagram of the experimental setup and (b) Experimental platform.

techniques are implemented in Simulink and embedded into the DSP by using Matlab2017b/Simulink and C2000 Code Generation Tools v6.0.0 software. The results are observed in a digital storage oscilloscope (Rigol DS1054Z) connected to Digital to Analog Converter (DAC) module.

Experimental results for Test-I using the hardware setup (Fig. 8) are given in 9. Results in Fig. 9 show that the proposed technique converged in under a cycle and the convergence time is ≈ 2 times faster than the comparative techniques. This shows that the proposed technique has fast dynamic response. Test-II in Sec. IV-A considered voltage swell. Similar to voltage swell, voltage sag is also not so uncommon in power grid. Experimental results for -0.5p.u. voltage sag are given in Fig. 10. Waveforms in Fig. 10 show that the voltage sag occur when the voltage is at the positive peak. This is a very challenging situation. Experimental results in 10 show that the proposed technique has the fastest convergence time even in this challenging condition. This validates the performance of the proposed technique in the case of sudden large dip in grid voltage.

In Sec. IV-A, performance of the proposed MAO has been tested under distorted grid voltage condition. In that test, we assumed that the harmonics are known. However, in practice, grid harmonics may not be known a priori. As a result, harmonics robustness of a single AO tuned at the fundamental frequency needs to be considered. Experimental results in the presence of distorted grid voltage is given in Fig.11. Experimental results in Fig. 11 show that the fast convergence of the proposed technique doesn't come at the cost of sacrificing harmonic robustness. Moreover, the THD of the proposed technique is 2.75% which is well under the 5% limit set by the European standard EN 50160 for grid integration of distributed energy sources. This is a significant advantage of the proposed technique over the comparative techniques.

V. CONCLUSION

In this paper, a frequency adaptive linear observer has been proposed to estimate the phase and frequency of a single-phase grid voltage signal. By proposing a novel parametrized linear dynamical model of the grid voltage signal, a linear observer is proposed. The observer depends on the accurate value of the grid frequency parameter. A nonlinear adaptation law is proposed for the adaptive frequency adaptation. The proposed technique is theoretically sound with local stability proof, easy to realize in practical hardware and provides fast and accurate estimation of phase and frequency. As no filtering is needed, trade-off between good dynamic response and bandwidth is not that important for our technique. This makes the proposed technique very suitable for industrial applications.

References

[1] M. Parvez, M. F. M. Elias, F. Blaabjerg, D. Abbott, and S. F. Al-Sarawi, "Comparative study of discrete PI and PR controls for single-phase UPS inverter," *IEEE Access*, vol. 8, pp. 45 584 – 45 595, 2020.

[2] A. Ahmad, N. Ullah, N. Ahmed, A. Ibeas, G. Mehdi, J. Herrera, and A. Ali, "Robust control of grid-tied parallel inverters using nonlinear backstepping approach," *IEEE Access*, vol. 7, pp. 111 982–111 992, 2019.

[3] U. K. Shinde, S. G. Kadwane, S. Gawande, M. J. B. Reddy, and D. Mohanta, "Sliding mode control of single-phase grid-connected quasi-Z-source inverter," *IEEE Access*, vol. 5, pp. 10 232–10 240, 2017.

[4] A. E. Leon, J. M. Mauricio, J. A. Solsona, and A. Gomez-Exposito, "Software sensor-based STATCOM control under unbalanced conditions," IEEE Trans Power Del, vol. 24, no. 3, pp. 1623–1632, Jul. 2009.

[5] L. Guo, N. Jin, Y. Li, and K. Luo, "A model predictive control method for grid-connected power converters without ac voltage sensors," *IEEE Trans. Ind. Electron.*, early access, Feb. 05, 2020. [Online]. Available: https://doi.org/10.1109/TIE.2020.2970638

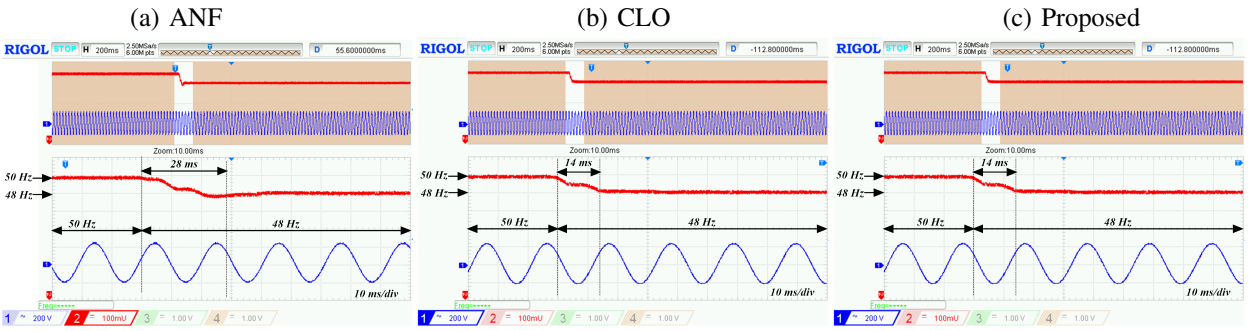

Figure 9: Comparative experimental results for -2 Hz step change in frequency.

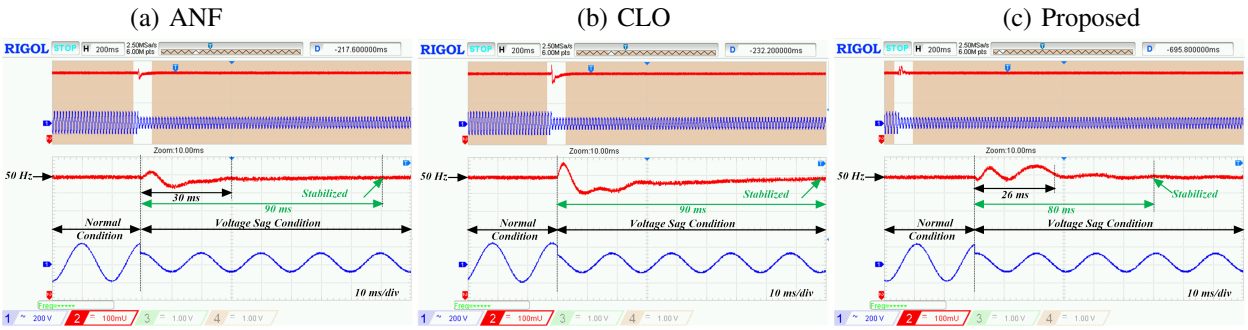

Figure 10: Comparative experimental results for -0.5 p.u. step change in voltage.

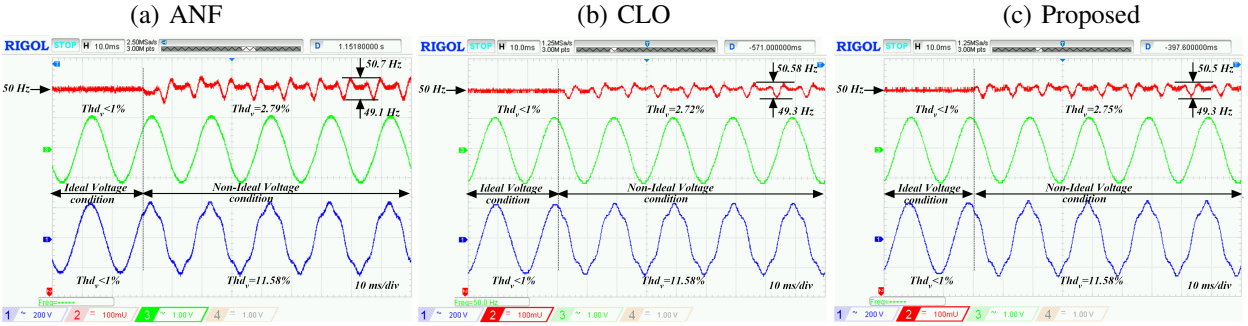

Figure 11: Comparative experimental results for ideal to distorted grid voltage transition.

[6] S. Biricik, H. Komurcugil, N. D. Tuyen, and M. Basu, "Protection of sensitive loads using sliding mode controlled three-phase DVR with adaptive notch filter," *IEEE Trans. Ind. Electron.*, vol. 66, no. 7, pp. 5465–5475, Jul. 2018.

[7] A. Rahoui, A. Bechouche, H. Seddiki, and D. O. Abdeslam, "Grid voltages estimation for three-phase PWM rectifiers control without AC voltage sensors," *IEEE Trans. Power Electron.*, vol. 33, no. 1, pp. 859–875, Jan. 2018.

[8] Y. Zhang, Z. Wang, J. Jiao, and J. Liu, "Grid-voltage sensorless model predictive control of three-phase pwm rectifier under unbalanced and distorted grid voltages," *IEEE Trans. Power Electron.*, early access, Dec. 31, 2019. [Online]. Available: https://doi.org/10.1109/TPEL.2019.2963206

[9] M. S. Reza, M. Ciobotaru, and V. G. Agelidis, "Accurate estimation of single-phase grid voltage parameters under distorted conditions," *IEEE Trans. Power Del.*, vol. 29, no. 3, pp. 1138–1146, Jun. 2014.

[10] S. Reza, M. Ciobotaru, and V. G. Agelidis, "Accurate estimation of single-phase grid voltage fundamental amplitude and frequency by using a frequency adaptive linear Kalman filter," *IEEE Trans. Emerg. Sel. Topics Power Electron.*, vol. 4, no. 4, pp. 1226–1235, Dec. 2016.

[11] N. Kumar, B. Singh, and B. K. Panigrahi, "Integration of solar PV with low-voltage weak grid system: Using maximize-M Kalman filter and self-tuned P&O algorithm," *IEEE Trans. Ind. Electron.*, vol. 66, no. 11, pp. 9013–9022, Nov. 2019.

[12] P. D. Achlerkar and B. K. Panigrahi, "Recursive least squares based adaptive parameter estimation scheme for signal transformation and grid synchronization," *IEEE Trans. Emerg. Sel. Topics Power Electron.*, early access, Jan. 30, 2020. [Online]. Available: https://doi.org/10.1109/JESTPE.2020.2970445

[13] Y. Terriche, J. M. Guerrero, and J. C. Vasquez, "Performance improvement of shunt active power filter based on non-linear least-square approach," *Electr. Power Syst. Res.*, vol. 160, pp. 44–55, Jul. 2018.

[14] S. Mekhilef, M. Tarek, and N. Abd. Rahim, "Single-phase hybrid active power filter with adaptive notch filter for harmonic current estimation," *IETE Journal of Research*, vol. 57, no. 1, pp. 20–28, 2011.

[15] M. S. Reza, F. Sadeque, M. M. Hossain, A. M. Ghias, and V. G. Agelidis, "Three-phase PLL for grid-connected power converters under both amplitude and phase unbalanced conditions," *IEEE Trans. Ind. Electron.*, vol. 66, no. 11, pp. 8881–8891, Nov. 2019.

[16] M. S. Reza, M. M. Hossain, and A. M. Ghias, "Open-loop approach for robust detection of selective harmonic in single-phase system," *IEEE Trans. Ind. Informat.*, vol. 15, no. 12, pp. 6260–6269, Dec. 2019.

[17] Y. Terriche, M. U. Mutarraf, M. Mehrzadi, A. Lashab, J. M. Guerrero, J. C. Vasquez, and D. Kerdoun, "Adaptive CDSC-based open-loop synchroniza-

tion technique for dynamic response enhancement of active power filters," *IEEE Access*, vol. 7, pp. 96 743–96 752, 2019.
[18] M. Chen, L. Peng, B. Wang, and W. Wu, "Accurate and fast harmonic detection based on the generalized trigonometric function delayed signal cancellation," *IEEE Access*, vol. 7, pp. 3438–3447, 2019.
[19] S. Wang, A. Etemadi, and M. Doroslovački, "Adaptive cascaded delayed signal cancellation pll for three-phase grid under unbalanced and distorted condition," *Electr. Power Syst. Res.*, vol. 180, p. 106165, 2020.
[20] H. Ahmed, M. Benbouzid, M. Ahsan, A. Albarbar, and M. Shahjalal, "Frequency adaptive parameter estimation of unbalanced and distorted power grid," *IEEE Access*, vol. 8, pp. 8512 – 8519, 2020.
[21] Z. Dai, W. Lin, and H. Lin, "Estimation of single-phase grid voltage parameters with zero steady-state error," *IEEE Trans. Power Electron.*, vol. 31, no. 5, pp. 3867–3879, May 2016.
[22] Z. Dai and W. Lin, "Adaptive estimation of three-phase grid voltage parameters under unbalanced faults and harmonic disturbances," *IEEE Trans. Power Electron.*, vol. 32, no. 7, pp. 5613–5627, July 2017.
[23] H. Ahmed, S.-A. Amamra, and I. Salgado, "Fast estimation of phase and frequency for single-phase grid signal," *IEEE Trans. Ind. Electron.*, vol. 66, no. 8, pp. 6408–6411, Aug. 2019.
[24] A. Kherbachi, A. Chouder, A. Bendib, K. Kara, and S. Barkat, "Enhanced structure of second-order generalized integrator frequency-locked loop suitable for DC-offset rejection in single-phase systems," *Electr. Power Syst. Res.*, vol. 170, pp. 348–357, 2019.
[25] M. L. Pay and H. Ahmed, "Modeling and tuning of circular limit cycle oscillator fll with preloop filter," *IEEE Trans. Ind. Electron.*, vol. 66, no. 12, pp. 9632–9635, Dec. 2019.
[26] Z. Chedjara, A. Massoum, S. Massoum, P. Wira, A. Safa, and A. Gouichiche, "A novel robust PLL algorithm applied to the control of a shunt active power filter using a self tuning filter concept," in *2018 IEEE International Conference on Industrial Technology (ICIT)*. IEEE, 2018, pp. 1124–1131.
[27] A. A. Ahmad, M. Pichan, and A. Abrishamifar, "A new simple structure PLL for both single and three phase applications," *International Journal of Electrical Power & Energy Systems*, vol. 74, pp. 118–125, 2016.
[28] M. Karimi-Ghartemani, *Enhanced phase-locked loop structures for power and energy applications*. John Wiley & Sons, 2014.
[29] M. E. Meral and D. Çelik, "Benchmarking simulation and theory of various PLLs produce orthogonal signals under abnormal electric grid conditions," *Electrical Engineering*, vol. 100, no. 3, pp. 1805–1817, 2018.
[30] M. Ciobotaru, R. Teodorescu, and F. Blaabjerg, "A new single-phase PLL structure based on second order generalized integrator," in *Power Electronics Specialists Conference, 2006. PESC'06. 37th IEEE*. IEEE, 2006, pp. 1–6.
[31] H. Ahmed and M. Benbouzid, "Demodulation type single-phase PLL with DC offset rejection," *Electron. Lett.*, vol. 56, no. 7, pp. 344–347, 2020.
[32] K. Mathuria, I. Hussain, B. Singh, and N. Kumar, "A quadrature oscillator-based DT for accurate estimation of fundamental load current for PV system in distribution network," *IEEE Trans. Ind. Informat.*, vol. 15, no. 6, pp. 3324–3333, Jun. 2018.
[33] A. K. Verma, R. K. Jarial, P. Roncero-Sanchez, M. R. Ungarala, and J. M. Guerrero, "An improved hybrid pre-filtered open-loop algorithm for three-phase grid synchronization," *IEEE Trans. Ind. Electron.*, Feb. 26, 2020.
[34] A. Safa, E. M. Berkouk, Y. Messlem, Z. Chedjara, and A. Gouichiche, "A pseudo open loop synchronization technique for heavily distorted grid voltage," *Electr. Power Syst. Res.*, vol. 158, pp. 136–146, 2018.
[35] M. Karimi-Ghartemani, "A unifying approach to single-phase synchronous reference frame PLLs," *IEEE Trans. Power Electron.*, vol. 28, no. 10, pp. 4550–4556, Oct. 2013.
[36] R. Burden, J. Faires, and A. Reynolds, *Numerical Analysis*, 2nd ed. Prindle, Weber and Schmidt, 1981.
[37] M. Karimi-Ghartemani, S. A. Khajehoddin, P. K. Jain, A. Bakhshai, and M. Mojiri, "Addressing DC component in PLL and notch filter algorithms," *IEEE Trans. Power Electron.*, vol. 27, no. 1, pp. 78–86, Jan. 2012.
[38] C. M. Hackl and M. Landerer, "A unified method for online detection of phase variables and symmetrical components of unbalanced three-phase systems with harmonic distortion," *Energies*, vol. 12, no. 17, p. 3243, 2019.
[39] H. Ahmed, S.-A. Amamra, and M. Bierhoff, "Frequency-locked loop based estimation of single-phase grid voltage parameters," *IEEE Trans. Ind. Electron.*, vol. 66, no. 11, pp. 8856–8859, Nov 2019.

HAFIZ AHMED (S'10–M'17) received the B.Sc. degree in Electrical & Electronic Engineering from Ahsanullah University of Science and Technology, Dhaka, Bangladesh, in 2011, the M.Sc. degree in Systems, Control and Information Technology from Joseph Fourier University, Grenoble, France, in 2013, and the Ph.D. degree in Automatic Control from the University of Lille 1, France, in 2016.

For the Ph.D. thesis, he received the EECI (European Embedded Control Institute) Ph.D. award, 2017. He has also obtained the Best PhD Theses award from the Research Cluster on Modeling, Analysis and Management of Dynamic Systems (GDR-MACS) of the National Council of Scientific Research (CNRS) in France in 2017. He was a Postdoctoral fellow at Clemson University, SC, USA followed by academic appointments in Bangladesh at the University of Asia Pacific and North South University. Since September 2017, he joined the School of Mechanical, Aerospace and Automotive Engineering, Coventry University, United Kingdom. He is interested in applied control engineering with special focus in energy and environment. He is an Associate Editor of the INTERNATIONAL JOURNAL OF ELECTRICAL ENGINEERING & EDUCATION.

MOMINUL AHSAN is a Postdoctoral Researcher in the Department of Engineering, Manchester Met University. He completed his PhD degree in 2019 from the School of Computing and Mathematical Sciences at University of Greenwich, London, UK. Mr. Ahsan has obtained his MEng degree (Research) from the Faculty of Engineering and Computing at Dublin City University, Dublin, Ireland in 2014 and Bachelor Degree from the Department of Computer Science and Engineering at State University of Bangladesh, Dhaka, Bangladesh in 2008. Mominul's research interests include prognostics, data analytics, machine learning, reliability, power electronics, wireless communication and wearable technology.

Dr. Ahsan is currently a Member of Institution of Engineering and Technology (MIET) UK, Associate Fellow of Higher Education Academy (AFHEA) UK and Associate Member of Bangladesh Computer Society. He is also a recipient of MEng stipend at Dublin City University in 2010, PhD scholarship at University of Greenwich in 2014 and Excellent Poster Award in the IEEE International Spring Seminar on Electronic Technology at Sofia, Bulgaria in 2017.

MOHAMED BENBOUZID (S'92–M'95–SM'98–F'20) received the B.Sc. degree in electrical engineering from the University of Batna, Batna, Algeria, in 1990, the M.Sc. and Ph.D. degrees in electrical and computer engineering from the National Polytechnic Institute of Grenoble, Grenoble, France, in 1991 and 1994, respectively, and the Habilitation à Diriger des Recherches degree from the University of Picardie "Jules Verne," Amiens, France, in 2000.

After receiving the Ph.D. degree, he joined the Professional Institute of Amiens, University of Picardie "Jules Verne," where he was an Associate Professor of electrical and computer engineering. Since September 2004, he has been with the University of Brest, Brest, France, where he is a Full Professor of electrical engineering. Prof. Benbouzid is also a Distinguished Professor and a 1000 Talent Expert at the Shanghai Maritime University, Shanghai, China. His main research interests and experience include analysis, design, and control of electric machines, variable-speed drives for traction, propulsion, and renewable energy applications, and fault diagnosis of electric machines.

Prof. Benbouzid has been elevated as an IEEE Fellow for his contributions to diagnosis and fault-tolerant control of electric machines and drives. He is also a Fellow of the IET. He is the Editor-in-Chief of the INTERNATIONAL JOURNAL ON ENERGY CONVERSION and the APPLIED SCIENCES (MDPI) Section on Electrical, Electronics and Communications Engineering. He is a Subject Editor for the IET RENEWABLE POWER GENERATION. He is also an Associate Editor of the IEEE TRANSACTIONS ON ENERGY CONVERSION.

ALHUSSEIN ALBARBAR is a Reader at the Department of Engineering, Manchester Met University. He has well over 27 years of industrial working experience and as an academic active researcher. Alhussein led and participated in over $7M of major projects and supervised over 21 research degrees including 15 doctoral studies. He has published 3 books, 5-book chapters, over 100 technical papers in refereed journals and international conference proceedings. His current research activities include Industry 4.0 applications, renewable power systems, smart sensing, intelligent control and monitoring algorithms used for electromechanical power plants.

MOHAMMAD SHAHJALAL received the B.Sc. degree in electrical and electronics engineering from Chittagong University of Engineering and Technology, Bangladesh, in 2009, the M.Sc. degree in digital image and signal processing from the university of Manchester, Manchester, United Kingdom, in 2013, and the Ph.D. degree in computing and mathematical sciences from University of Greenwich , Greenwich, United Kingdom, in 2018. He was a lecturer with the Department of Electrical and Electronics Engineering, International Islamic University of Chittagong, Bangladesh, in 2010-2012. Since 2018 he has been leading the project titled thermal characterisation of li-ion pouch cells employed in Jaguar's first electric car I-PACE in WMG. His current research interests include electro-thermal modelling, packaging, and reliability of power electronic systems and components and reversible heat characterisation and quantification of energy storage systems of electric vehicle.

SAMET BIRICIK (M'12–SM'19) received the B.Sc., M.Sc., and Ph.D. degrees in electrical and electronic engineering from the Near East University, Nicosia, Mersin 10, Turkey, in 2006, 2009, and 2013, respectively. He is currently a lecturer in the European University of Lefke, Lefke and a Research Fellow in the School of Electrical and Electronic Engineering of Technological University Dublin, Dublin, Ireland. His research interests include the application of power electronics, power quality, electrical machines, and high-voltage engineering.